Articles

Chemical and Structural Probing of the N-Terminal Residues Encoded by *FMR1* Exon 15 and Their Effect on Downstream Arginine Methylation[†]

Natalia Dolzhanskaya,[‡] David C. Bolton,[§] and Robert B. Denman*[,‡]

Department of Molecular Biology, New York State Institute for Basic Research in Developmental Disabilities, 1050 Forest Hill Road, Staten Island, New York 10314

Received November 20, 2007; Revised Manuscript Received June 3, 2008

ABSTRACT: Exon 15 of the fragile X mental retardation protein gene (FMR1) is alternatively spliced into three variants. The amino acids encoded by the 5′ end of the exon contain several regulatory determinants including phosphorylation sites and a potential conformational switch. Residues encoded by the 3′ end of the exon specify FMRP's RGG box, an RNA binding domain that interacts with G-quartet motifs. Previous studies demonstrated that the exon 15-encoded N-terminal residues influence the extent of arginine methylation, independent of S_{500} phosphorylation. In the present study we focus on the role the putative conformational switch plays in arginine methylation. Chemical and structural probing of Ex15 alternatively spliced variant proteins and several mutants leads to the following conclusions: Ex15c resides largely in a conformation that is refractory toward methylation; however, it can be methylated by supplementing extracts with recombinant PRMT1 or PRMT3. Protein modeling studies reveal that the RG-rich region is part of a three to four strand antiparallel β-sheet, which in other RNA binding proteins functions as a platform for nucleic acid interactions. In the Ex15c variant the first strand of this sheet is truncated, and this significantly perturbs the side-chain conformations of the arginine residues in the RG-rich region. Mutating R_{507} in the conformational switch to K also truncates the first strand of the β-sheet, and corresponding decreases in *in vitro* methylation were found for this and R_{507}/R_{544} and R_{507}/R_{546} double mutants. These effects are not due to the loss of R_{507} methylation as a conformational switch-containing peptide reacted under substrate excess and in methyl donor excess was not significantly methylated. Consistent with this, similar changes in β-sheet structure and decreases in *in vitro* methylation were observed with a W_{513}-K mutant. These data support a novel model for FMRP arginine methylation and a role for conformational switch residues in arginine modification.

The protein arginine methyltransferases (PRMTs),[1] a subfamily of methyltransferase enzymes, now numbering 11 members (*1, 2*), catalyze the transfer of methyl groups from *S*-adenosylmethionine to target proteins. Dimerization, a conserved feature of these proteins (*3*), is a necessary requirement for methylation (*4, 5*); however, *in vivo* the enzymes are found as large homooligomeric complexes (*6*) and as part of large multisubunit complexes (*7–9*). In general, there are two broad classes of PRMT substrates: histones (*10–13*) and associated chromatin remodeling complexes (*14*) and nonhistone proteins, the bulk of which are RNA binding proteins (RBPs) (*15–24*).

The fragile X mental retardation protein (FMRP), a prototypical member of the heterogeneous nuclear ribonucleoprotein K (hnRNPK) family of RNA binding proteins (*25*), contains a C-terminal arginine−glycine-rich region (RG-rich) (*26*) that is a prime site for PRMT modification (*27, 28*). Not surprisingly, therefore, FMRP's RG-rich region has been found to be methylated both *in vitro* and *in vivo* (*29–33*), and methylation has been shown to affect both its protein−protein and protein−RNA interactions.

Recent work has also shown that alternative splicing just upstream of sequences that encode FMRP's RG-rich region produces three protein variants that are differentially methylated *in vitro* (*31*). The largest variant encodes a conservative phosphorylation site (S_{500}) (*34*), and its phosphorylation negatively regulates the translation of FMRP-bound

[†] These studies were generously supported by the New York State Research Foundation for Mental Hygiene and the FRAXA Foundation.

* Corresponding author. Tel: (718) 494-5199. Fax: (718) 494-5905. E-mail: rbdenman@yahoo.com.

[‡] Biochemical Molecular Neurobiology Laboratory.

[§] Molecular Structure and Function Laboratory.

[1] Abbreviations: 53BP1, p53 binding protein 1; CARM1, coactivator-associated arginine methyltransferase 1; CD, circular dichroism; DMC, dimethylcarbodiimide; FMR1, fragile X mental retardation protein mRNA; FMRP, fragile X mental retardation protein; $FMRP_{Ex15x}$, FMRP exon 15 alternatively spliced full-length protein variant; Ex15x, FMRP exon 15 truncated protein; FXS, fragile X syndrome; hnRNPK, heterogeneous nuclear ribonucleoprotein K; KH, hnRNPK homology RNA binding domain; LC-MS, liquid chromatography coupled mass spectrometry; mAb, monoclonal antibody; MMA, monomethylarginine; mRNP, messenger ribonucleoprotein particle; MBP, myelin basic protein; MSP58, microspherule protein; MT, methyltransferase; NBS, *N*-bromosuccinimide; pAb, polyclonal antibody; PG, phenylglyoxal; PRMT1, protein arginine methyltransferase 1; PRMT3, protein arginine methyltransferase 3; PRMT4, protein arginine methyltransferase 4; Qtof, quadrapole time of flight; RBPs, RNA binding proteins; RGG box, RNA binding domain comprised of repeated RGG amino acid triads; RG-rich, arginine−glycine-rich region; RRL, rabbit reticulocyte lysate; SAM, *S*-adenosylmethionine; SAH, *S*-adenosylhomocysteine; sme, symmetrically dimethylated arginine.

10.1021/bi702298f CCC: $40.75
Published on Web 07/26/2008

Table 1: FMRP Exon 15 Mutants Used in These Studies

isoform	background	mutant	ref
$FMRP_{Ex15a}$	full length		*31*
$FMRP_{Ex15a}$	full length	$I_{304}N$	this study
$FMRP_{Ex15a}$	full length	$R_{507}K$	this study
$FMRP_{Ex15a}$	full length	$R_{546}K$	this study
Ex15a	truncation		*31*
Ex15a	truncation	$R_{507}K$	this study
Ex15a	truncation	$W_{513}K$[a]	this study
Ex15a	truncation	$R_{544}K$	*31*
Ex15a	truncation	$R_{546}K$	*31*
Ex15a	truncation	$R_{507}K/R_{544}K$	this study
Ex15a	truncation	$R_{507}K/R_{546}K$	this study
Ex15a	truncation	$W_{513}K/R_{546}K$[a]	this study
Ex15b	truncation		*31*
Ex15c	truncation		*31*

[a] These mutants were prepared by Bridgene Biotechnology, Inc.

mRNAs (*35*). Unlike some RG-rich proteins, however, phosphorylation and methylation appear not to be antagonistic in FMRP (*36, 37*). Nevertheless, the striking loss of methylation of the smallest variant, which lacks all possible upstream regulatory elements, suggested a role for these upstream residues. A common element of the two larger alternatively spliced variants that appear to be equally methylated *in vitro* is a short sequence (DHRDELSDW) that has been modeled as an unstructured region approximating a conformational switch (*38*). Therefore, it was of interest to determine the relationship between these residues and FMRP methylation as variant expression and posttranslational methylation may play a role in translational regulation at the synapse (*31*). Here we report the results of studies of select exon 15-encoded N-terminal site-directed mutants using protein modeling, chemical modification, and enzymatic assays.

EXPERIMENTAL PROCEDURES

Antibodies. V5 mAb was purchased from Invitrogen. HRP-conjugated secondary antibodies were purchased from Sigma. Alexa Fluor-conjugated secondary antibodies were purchased from Molecular Probes.

Proteins and Peptides. Recombinant PRMT1 and recombinant CARM1/PRMT4 were purchased from UpState. Recombinant PRMT3 was a generous gift of François Bachand, Department of Biochemistry, Université de Sherbrooke, Québec, Canada. Myelin basic protein fragment ($MBP_{104-118}$) was purchased from Sigma. Histone $H4(R_3)^{sme}$ peptide ($SGR^{sme}GKGGKGC-(NH_2)$) containing symmetrically dimethylated R_3 and histone H4(Ctrl) peptide (KRHRKVLRDNGGC-(OH)) were obtained from Abcam. $FMRP_{498-513}$ peptide was synthesized by CPC Scientific. The MGRGRTSSKELA control peptide used in the NBS studies was synthesized by Sigma GenoSys.

Buffers. HMTase buffer is 50 mM Tris-HCl, pH 9.0, 1 mM PMSF, and 0.5 mM DTT as previously described (*31, 39*).

Plasmids. The FMRP expression plasmid pET21A-hFMRP ($FMRP_{Ex15a}$) (*40*), pmHis-FMRP ($FMRP_{Ex15c}$) (*41*), and plasmid clones expressing *FMR1* exons 15−17 to the TGA stop codon (Ex15a, Ex15b, and Ex15c) (*31*) have been described. Mutations on an Ex15a background were constructed using a QuikChange site-directed mutagenesis kit according to the manufacturer's instructions (Stratagene). All plasmids (Table 1) were sequenced to verify their composition and transfected into PC12 cells to verify protein expression (Supporting Information Figure 1).

In Vitro Methylation Assays. Posttranslational in vitro methylation by recombinant PRMT1, PRMT3, CARM1/PRMT4 or the endogenous PRMTs in RRL was performed on *in vitro* translated proteins. Briefly, 5 μL aliquots of RRL-translation products were incubated in (HMTase buffer) supplemented with 1 μCi of ^{3}H-SAM and 2.5 μL of the respective PRMT in a total volume of 20 μL according to the manufacturer's instructions. Mock reactions contained all components except the recombinant PRMT. Incubations were allowed to proceed for 10 min to 2 h at 30 °C. Following the incubation an equal volume of 2× Laemelli sample buffer was added, and the samples were boiled for 5 min. The proteins were resolved by SDS−PAGE and processed for fluorography as previously described (*31, 42*).

Peptide assays in limiting methylation conditions were performed in a total volume of 20 μL solution consisting of 1× HMTase buffer supplemented with 0.5−1 μCi of ^{3}H-SAM, 300 pmol of peptide or 65 pmol of protein, 100 ng of recombinant PRMT1, 100 ng of recombinant CARM1/PRMT4, or 5−10 μL of RRL. Reactions were initiated by the addition of the methyltransferase and were allowed to proceed for 90 min at 30 °C. Under these conditions, less than 10% of the protein was methylated. At the end of the incubation, a 5 μL aliquot of the reaction mixture was withdrawn and spotted on a P81 membrane. The partially dried membranes were washed with 5 mL of 10% trifluoroacetic acid and subsequently with 5 mL of 95% ethanol. The membranes were transferred to vials containing 15 mL of Filtron-X (National Diagnostic Laboratories), and the retained radioactivity was measured in a scintillation counter. Background values were measured in mock reactions containing all of the components except the methyltransferase and were subtracted from the sample values.

For mass spectrometry 300 pmol of peptide was reacted with a 1250-fold molar excess of unlabeled SAM (Sigma) and 5 μL of RRL in a total volume of 20 μL of 1× HMTase buffer as described above. Reactions were allowed to proceed for 120 min at 30 °C.

Quantification of the kinetic studies was performed as follows. Each protein was assessed at least three times. A wild-type FMRP was always run in parallel as a control. Fluorogram intensities were measured with IPLab Gel software. For each fluorogram the wild-type FMRP intensity at 90 min was arbitrarily set to 100%, and all of the values normalized to it. Variations in protein load were quantified by Western blotting and the values used to calculate a final normalized activity for each time.

Mass Spectrometry. Peptides from methylation reactions were initially captured on OMIX C18 tips (Varian) according to the manufacturer's procedure. Bound peptides were eluted in 0.1% formic acid in 95% acetonitrile/water and then vacuum-dried. The samples were dissolved in LC-MS grade water containing 0.1% formic acid to an approximate concentration of 5 pmol/μL, and approximately 25 pmol (5 μL) was separated on a C18 column (Waters BEH130) using a 29 min gradient of 3% to 50% acetonitrile in aqueous 0.1% formic acid at a flow rate of 250 nL/min. Mass spectra were collected on a Qtof Micro tandem mass spectrometer from 5 to 45 min in 480 ms scans from *m/z* 200 to 1990 with 0.1 s data transfer interleaves. Chromatograms showing the

elution profiles of the control, CARM/PRMT4-treated, and RRL-treated $FMRP_{498-513}$ peptides were produced by plotting the data from the 3+ ion envelopes covering the *m*/*z* ranges for the mass isomers containing zero to three ^{13}C atoms for the unmethylated (630.81−632.06 Da), monomethylated (635.43−636.78 Da), and dimethylated (640.10−641.42 Da) species. The plotted data were smoothed by the Savitzky−Golay method (*43*) using two smoothes and a three-scan window.

The $FMRP_{498-513}$ synthetic peptide was found to elute in a single major peak at 25.3 min, primarily as 3+ and 2+ ions in a ratio of ~3:1, respectively, by LC-MS. The 3+ ion centroid *m*/*z* (630.9279; 3.3 ppm error), the 2+ ion centroid *m*/*z* (945.9089; 18.9 ppm error), and the TOF transformed 1+ ion centroid mass (1890.7716; 1.4 ppm error) were within the acceptable margins of error. The structure of the $FMRP_{498-513}$ peptide was confirmed by MS/MS analysis of the 3+ ion. LC-MS data were scanned for evidence of monomethylated and dimethylated forms of $FMRP_{498-513}$ by plotting the 3+ and 2+ ion envelopes having *m*/*z*'s consistent with increased peptide masses of 14.01 and 28.03 Da, respectively. Ions in these ranges were found in all samples (control, CARM/PRMT4-treated, RRL-treated) regardless of the absence of a methyltransferase or the presence of the methyltransferase inhibitor SAH. Insufficient ions were present to determine the structure of these forms by MS/MS analysis. The fact that the amount of each putative methylated form decreased with treatment suggests that these are not methylated peptides but may be peptide synthesis artifacts. The increased masses observed are consistent with substitution errors such as Glu for Asp.

Protein Modification. Modification of tryptophan residues by *N*-bromosuccinimde (NBS) was accomplished using the procedure of Petrova et al. (*44*). Briefly, RRL-produced proteins were incubated in 50 mM NaOAc, pH 5.0, containing 1 mM NBS. The reaction was allowed to proceed for 30 min at room temperature and subsequently filtered through Sephadex G-25 preequilibrated in 1× HMTase buffer to remove the excess unreacted NBS. The degree of modification was followed by measuring the decrease in A_{280} absorbance. The results were plotted as the ratio A/A_0 versus time. The modified protein was subjected to posttranslational methylation as described above.

Modification of arginine residues by phenylglyoxal (PG) was accomplished using the procedure of Takahashi (*45*). Briefly, RRL-produced proteins were incubated in 0.1 M Tris-HCl, pH 8.0, containing 1.5% PG. The reaction was allowed to proceed for 30 min at room temperature and subsequently filtered through Sephadex G-25 preequilibrated in 1× HMTase buffer to remove the excess unreacted PG. The modified protein was subjected to posttranslational methylation as described above.

Protein Modeling. Proteins were modeled using the HMMSTR/ROSETTA Monte Carlo fragment insertion folding program (http://www.bioinfo.rpi.edu/~bystrc/hmmstr/server.php). PDB files containing the best structure of each modeled variant were analyzed using DeepView/Swiss pdb viewer v3.7 (www.expasy.org/spdbv); the resulting output was converted into TIFF images for presentation. Amino acid accessibility was computed by DeepView/Swiss pdb viewer v3.7 and presented as a graded color scale.

RESULTS

Ex15c Methylation Is Enhanced by Exogenous PRMTs. FMR1 exon 15 is alternatively spliced *in vivo* (*46, 47*), resulting in three variants encoding proteins $FMRP_{Ex15a}$, $FMRP_{Ex15b}$, and $FMRP_{Ex15c}$ (Figure 1A). In a previous study we showed that altering the N-terminal sequences of *FMR1* exon 15-encoded residues produced dramatic effects on posttranslational arginine methylation in the RG-rich region of FMRP *in vitro*. Specifically, truncation of 25 amino acids, as occurs in the smallest alternatively spliced variant, resulted in an 7-fold reduction in FMRP methylation by the PRMTs found in rabbit reticulocyte lysates (RRL) (*31*).

As analysis of the N-terminal sequence that is deleted in the exon 15c variant indicated the presence of a putative conformational switch (*38*), we hypothesized that the RG-rich residues in exon 15c-containing FMRP variants might reside primarily in a conformation that was refractory to PRMTs but that adding additional PRMTs to RRL might overcome this block. Therefore, we examined the effect of adding recombinant PRMT1, PRMT3, and CARM1/PRMT4 to RRL-produced Ex15c, a truncated protein that mimics the methylation of full-length $FMRP_{Ex15c}$ (*31*). RRL-produced Ex15a, whose methylation is unaltered by the addition of recombinant PRMTs, was simultaneously processed as a control. As expected, supplementing RRL with PRMT1, PRMT3, or CARM1/PRMT4 produced no further methylation of Ex15a than that induced by the RRL. Also as previously shown, RRL-induced methylation of Ex15c was about 7-fold less than that of Ex15a. Importantly, however, adding PRMT1 or PRMT3 to Ex15c significantly increased the extent of its methylation (Figure 2A). These results clearly establish that Ex15c methylation can be modulated by recombinant PRMT supplementation, indicating that the protein is in fact methylation competent. Second, Ex15c methylation was PRMT-specific since CARM1/PRMT4 addition had no effect. Finally, further addition of recombinant PRMT1 to Ex15c methylation reactions produced a dose-dependent increase in methylation (Figure 2B). These data are consistent with the hypothesis that the RG-rich region of Ex15c exists in equilibrium with a primary conformer that is unable to be methylated and a minor conformer that can be methylated.

Protein Modeling Reveals Local and Global Changes in Ex15 Proteins. We modeled the three alternatively spliced variant proteins, Ex15a, Ex15, and Ex15c, to gain structural insights into the effect the FMR1 exon 15-encoded N-terminal residues had on the RG-rich region of the protein (Figure 3 and Supporting Information Figures 2 and 3). We found both local and long-range changes occurred when the N-terminal amino acids were changed. Ex15a was represented as a sawtooth structure with an extended FMRP domain and a compact V5/His tag. The N-terminal region including the conformational switch was modeled as two helices interspersed between two unstructured elements, while the RG-rich region of the protein formed part of a three strand antiparallel β-sheet (Table 2). Interestingly, the guanidino groups of methylation substrate residues R_{539}, R_{544}, and R_{546} were partially buried and not completely accessible to solvent. Ex15b's RG-rich region was similar to Ex15a's; however, residues $F_{550}K_{551}$ were modeled as a turn rather

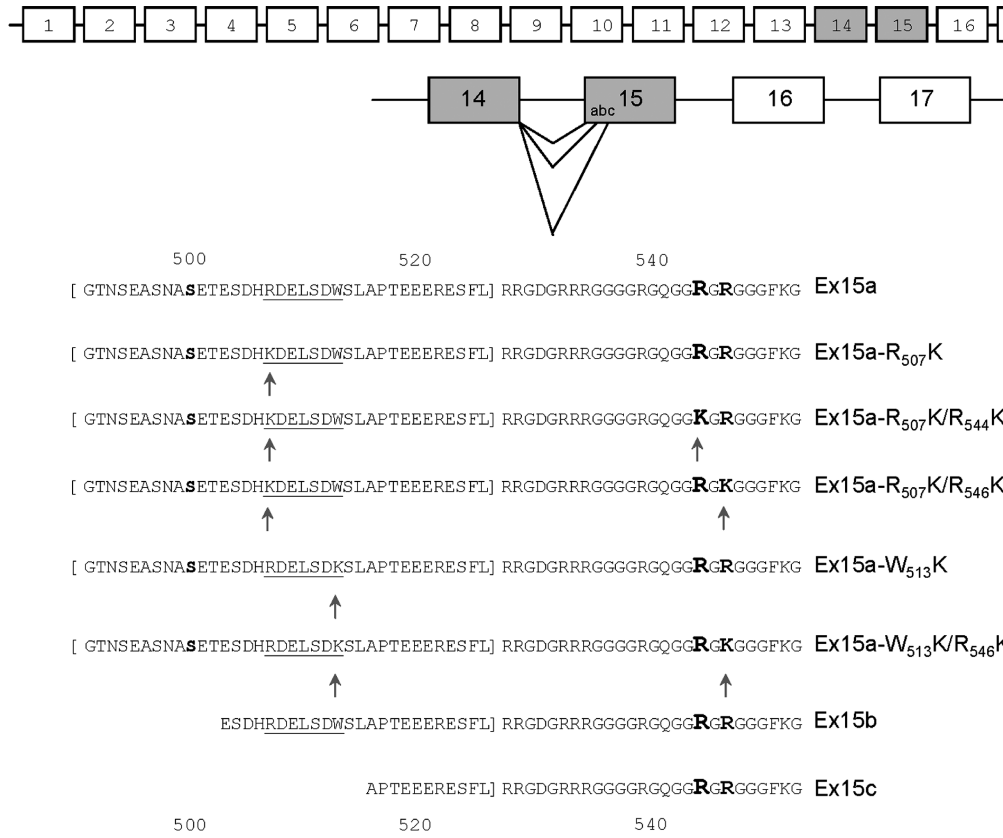

FIGURE 1: FMR1 exon 15 alternatively spliced variant proteins. (A) The schematic diagram (top) shows the 17 exons of FMR1 pre-mRNA as defined by Eichler et al. (*75*). Alternative splice site selection (bottom) occurring in exon 15 ultimately gives rise to three full-length variant proteins $FMRP_{Ex15a}$, $FMRP_{Ex15b}$, and $FMRP_{Ex15c}$. FMRP truncation expression plasmids (pEx15a, pEx15b, and pEx15c) encoding the three exon 15 splice site variants to the stop codon in exon 17 were previously described in Dolzahskaya et al. (*31*). (B) Exon 15a, 15b, 15c encoded residues of FMRP are shown. The conformational switch region is underlined; arginine residues R_{544} and R_{546} that are methylated by RRL are highlighted in bold. Mutant proteins used in these studies are similarly shown. The mutation sites are marked by arrows. The MSP58 binding site is set off in brackets.

than as a β-sheet. In addition, the overall shape of this molecule was globular.

The modeled structure of Ex15c differed in several respects from those of Ex15a and Ex15b. First, while the RG-rich region of Ex15c was modeled as a β-sheet, the N-terminal residues of the first strand of the sheet, which includes arginine residues $R_{532-534}$, were shortened compared to the Ex15a and Ex15b proteins (Table 2). Second, amino acids ESFLRR leading to the RG-rich region were modeled as a α-helix in Ex15a and Ex15b (Table 3); however, in the Ex15c model they are neither α-helix nor β-sheet. The net result of these changes is that the guanidino groups of methylation substrate residues R_{539}, R_{544}, and R_{546} become more solvent accessible in Ex15c.

These studies support the methylation results in Figure 2, suggesting that conformational changes in Ex15c influence the extent of arginine methylation.

Arginine Residues in Ex15c, but Not Ex15a or Ex15b, Are Modified by Phenylglyoxal. Chemical modification of specific amino acids is often used as a means of assessing critical protein residues. Among these is the selective modification of arginine by phenylglyoxal (PG) (*45*). We reasoned that if the modeling (above) was correct, the R residues in Ex15a and Ex15b, which are subject to methylation, might not be modified by PG. To test this hypothesis, we initially treated Ex15b with PG and compared its ability to be methylated with that of the untreated protein. The results of this experiment clearly show that PG pretreatment increased Ex15b methylation (Figure 4A). However, methylation of endogenous proteins in the RRL was negatively affected by PG treatment, indicating that PG modified those proteins. We then examined PG's effect on Ex15a and Ex15c methylation. As shown in Figure 4B, Ex15a methylation also increased following PG treatment (10%), while Ex15c exhibited a *ca.* 30% decrease compared to untreated samples. These data support the modeling predictions that the R residues in the RG-rich region of Ex15a and Ex15b are relatively inaccessible to solvent and that Ex15c's are slightly more exposed.

Posttranslational Methylation of RG-Rich Residues Is Altered in Exon 15a-R_{507}K Conformational Switch Mutants. To further explore the role the N-terminal residues encoded by FMR1 exon 15 play in arginine methylation, we prepared and examined several conformational switch mutants (Figure 1B). Initially, we examined the effect a conservative R-K mutation at position 507 (Ex15a numbering) had on the structure and methylation of Ex15a. Models of the R_{507}K mutation on an Ex15a background showed the RG-rich region of the molecule as part of a three strand antiparallel β-sheet. Interestingly, the location of the beginning of the first strand of the sheet aligns more closely with Ex15c than Ex15a (Table 2).

To determine whether the predicted conformational changes from the protein modeling studies correlated with changes in arginine methylation, we constructed this conformational switch mutant as well as several double mutants and tested

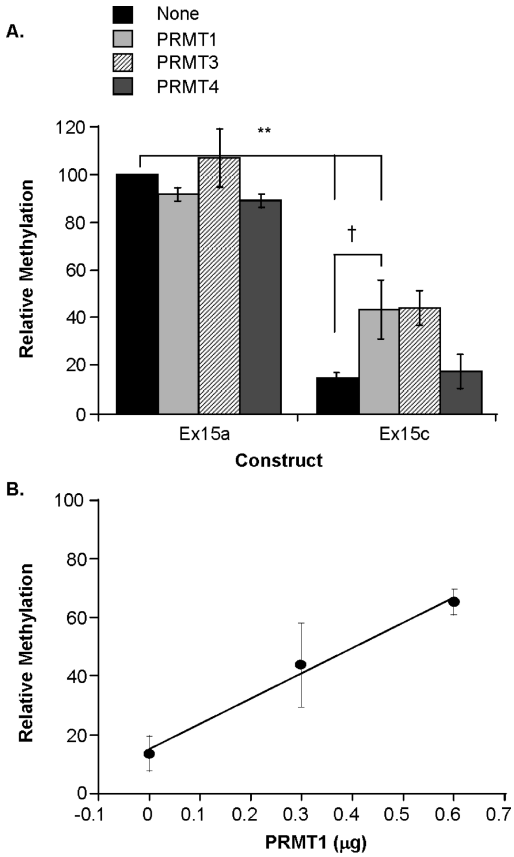

FIGURE 2: Recombinant PRMT1 and PRMT3 partially compensate for the methylation defect of Ex15c. (A) Posttranslational *in vitro* methylation of RRL-translated Ex15a and Ex15c was performed in the absence or presence of recombinant PRMTs, as indicated. Values for four to six reactions per protein per addition were normalized to the intensity of Ex15a methylation at 90 min without added recombinant PRMTs. Asterisk denotes $P < 0.0001$, one-way ANOVA, Scheffe's post hoc test; cross denotes $P = 0.005$, one-way ANOVA, Scheffe's post hoc test. (B) Effect of linear addition of recombinant PRMT1 on Ex15c methylation. The results of four to six reactions per concentration were normalized to the intensity of Ex15a at 90 min and plotted.

their ability to be posttranslationally methylated. The results of these studies show that the methylation of each of the point and double-point mutants was reduced compared to the Ex15a control (Figure 5A).

Interestingly, the $R_{507}K$ mutation was found to additively modulate the methylation of the double mutants. Previous work has shown that both R_{546} and R_{544} are methylated *in vitro* (*31, 48*) and *in vivo* (*33*); however, R_{507} was not assessed. The immediate context of R_{507}, i.e., HRD, as well as its greater context, i.e., SDHRDEL, does not resemble the PRMT1 and PRMT3 consensus motif FGGRGGF (*49*) or the loose consensus sequence of PRMT4, RPAAPR (*28*); thus it is not likely to be methylated. Nevertheless, to directly address this, we synthesized a 15-mer peptide corresponding to the N-terminal residues of FMRP exon 15a (NASETESDRDELSDW, $FMRP_{498-513}$) and conducted methylation assays with it and several controls. As shown in Figure 5B,C, recombinant proteins, PRMT1 and PRMT4, were unable to methylate $FMRP_{498-513}$. Recombinant PRMT1 weakly methylated Nola1, an RG-rich protein and known substrate of the enzyme (*50*), but was unable to methylate histone H3 or $MBP_{104-118}$, which are CARM1/PRMT4 substrates (*51*). Additionally, a histone H4 peptide containing a single R residue that is symmetrically dimethylated ($H4(R_3)^{sme}$) and another histone H4 peptide containing three R residues that are not known to be methylated (H4(Ctrl)) were not methylated by PRMT1. Recombinant CARM1/PRMT4 robustly modified histone H3 and $MBP_{104-118}$ and very weakly modified Nola1; however, it did not methylate either histone H4 peptide, as expected. Finally, when RRL was used as the source of PRMTs, Nola1 and MBP proteins were well methylated, but $FMRP_{498-513}$ and the histone H4 peptides were not (Figure 5D).

The posttranslational peptide methylation reactions described above were conducted with less than stoichiometric amounts of ^{3}H-SAM. Therefore, we next determined whether the $FMRP_{498-513}$ could be methylated in the presence of excess SAM. Using more than a 1000-fold molar excess of unlabeled SAM, we found less than 4% monomethylarginine and no dimethylarginine were incorporated into the peptide by liquid chromatography mass spectrometry (Figure 6A). In fact, this is probably an overestimate of the monomethylarginine content of the peptide (see Experimental Procedures). This is underscored by the fact that MS/MS analysis of the parent $FMRP_{498-513}$ peptide did not reveal the presence of either methyl-peptide fragments or other signature methylation ions (Figure 6B and Supporting Information Table 1). Nevertheless, when we analyzed $H4(R_3)^{sme}$, we observed the expected methylation signature ions, affirming our ability to detect methylated peptides (Supporting Information Figure 4 and Supporting Information Table 2).

We conclude from these studies that R_{507} is not methylated; therefore, the decreased methylation of the $R_{507}K$ mutants is most likely due to structural changes that affect the methylation of other arginine residues.

To determine whether the results of the methylation studies of the Ex15 conformational shift mutants faithfully reflect methylation in the full-length protein, a full-length construct containing the $R_{507}K$ mutation was prepared, and the ability of the RRL-produced protein ($FMRP_{Ex15a\text{-}R507K}$) to be methylated was compared to the wild-type protein ($FMRP_{Ex15a}$). As additional controls we also examined full-length proteins containing a $R_{546}K$ substitution and an $I_{304}N$ substitution, respectively. The latter is a naturally occurring mutation in the KH_1 RNA binding domain of FMRP, which gives rise to a very pronounced phenotype (*25, 52*). We found that, like Ex15a-$R_{507}K$, full-length $FMRP_{Ex15a\text{-}R507K}$ exhibited reduced methylation compared to the wild-type protein (Figure 7). Similarly, methylation of a full-length $FMRP_{Ex15a\text{-}R546K}$ was reduced compared to the full-length wild-type protein. For both, the magnitude of the reductions, *ca.* 40% and 15%, respectively, correlated with reductions seen in the truncation mutants. As this was also previously observed with comparisons of $FMRP_{Ex15a}$ and $FMRP_{Ex15c}$ and their corresponding truncation mutants (*31*), we conclude that these truncation proteins faithfully mimic the methylation properties of full-length FMRPs. Importantly, the decreased methylation of the full-length $R_{507}K$ mutant was specific since the $I_{304}N$ mutation had no effect on arginine methylation.

Posttranslational Methylation of RG-Rich Residues Is Also Altered in Exon 15a-$W_{513}K$ Conformational Switch Mutants. Tryptophan at position 513 in FMRP lies on the opposite end of the putative conformational switch. To extend the analysis of the effect that modifying this region has on arginine methylation truncation mutants, Ex15a-$W_{513}K$ and

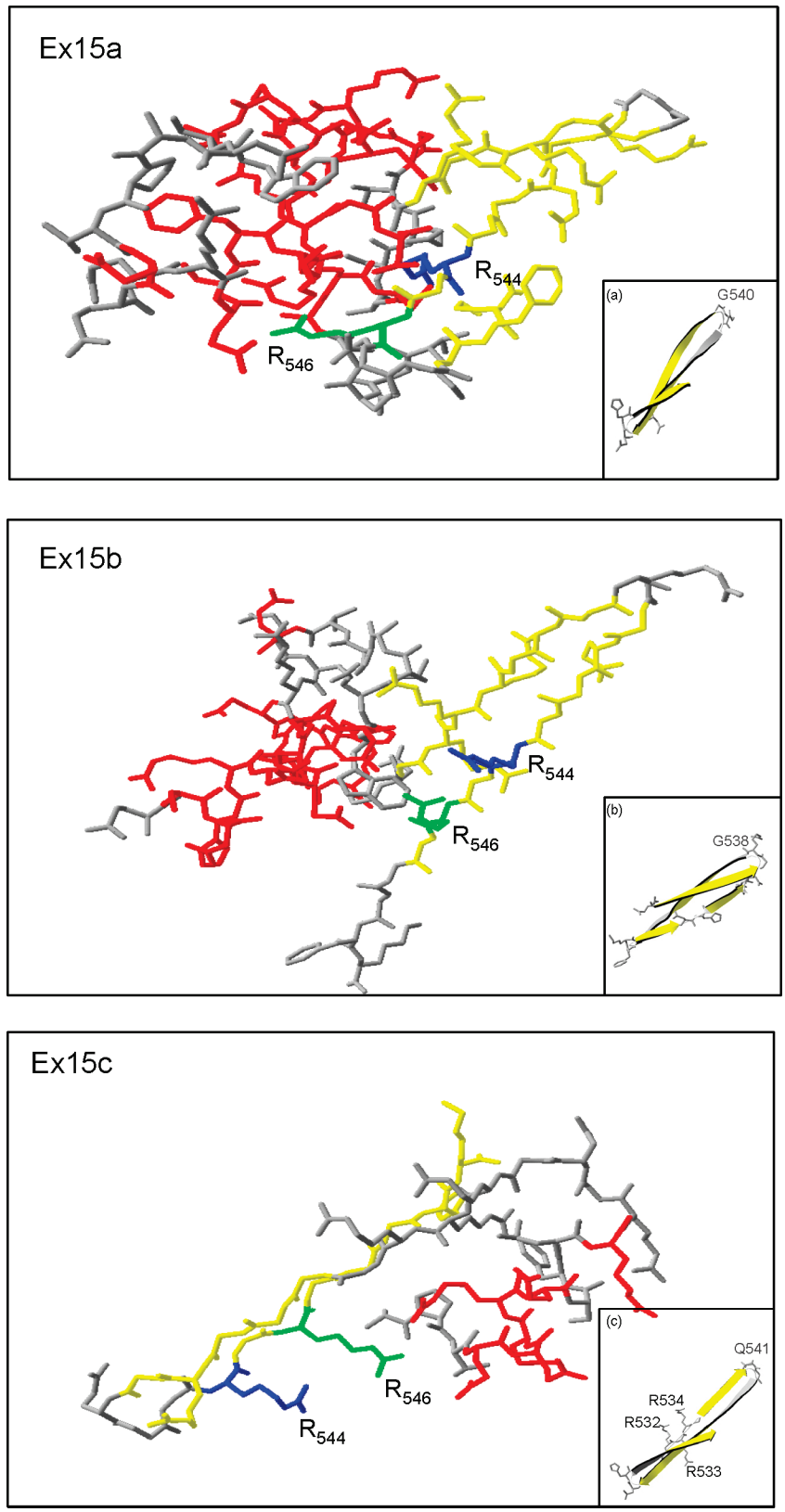

FIGURE 3: Ex15 alternatively spliced variant models exhibit variations in folding. (A) Ex15a, (B) Ex15b, and (C) Ex15c were modeled using the HMMSTR/ROSETTA Monte Carlo fragment insertion-folding program. Models of the lowest energy state for each of the truncated proteins are presented; they are uniformly oriented with the guanidino groups of R_{544} and R_{546} pointing to the right. For clarity only the exon 15-encoded residues are presented. (Complete views of the folded proteins are provided in Supporting Information Figure 2.) Here, helices are rendered in red and β-sheets in yellow; all else is in gray. For viewing purposes R_{544} is marked in blue and R_{546} is marked green although both are predicted to be in β-sheet conformation. Insets (a−c) show the three to four strand antiparallel β-sheet structure of which the RG-rich region is a part. In the models, the β-sheets are depicted in yellow as in the larger model while the turns are colored gray. Residues marking turn 2 (Table 1) in the structures of Ex15a, Ex15b, and Ex15c (G_{540}, G_{538} and Q_{541}, respectively) are marked in gray. The three arginine residues, which define the beginning of the RG-rich region ($R_{532-534}$), are shown in black. Note that $R_{532-534}$ in Ex15c is associated with a turn rather than the β-sheet. Full-sized images of each inset are provided in Supporting Information Figure 5.

Table 2: Location of Turns in the β-Sheet Encompassing FMRP's RG-Rich Region[a]

protein	turn 1	turn 2	turn 3	turn 4
Ex15a	$G_{529}D_{530}$	$G_{540}Q_{541}G_{542}$	none	$D_{555}H_{556}$
Ex15b	$G_{529}D_{530}$	$G_{538}R_{539}$	$F_{550}K_{551}$	$D_{555}H_{556}$
Ex15c	R_{528}-G_{535}	$Q_{541}G_{542}$	none	$D_{555}H_{556}$
Ex15a-$R_{507}K$	R_{532}-R_{534}	$G_{542}G_{543}$	none	$D_{555}H_{556}$
Ex15a-$R_{507}K/R_{546}K$	$R_{532}R_{533}$	$Q_{541}G_{542}$	none	$D_{555}H_{556}$
Ex15a-$W_{513}K$	$R_{534}G_{535}$	$Q_{541}G_{542}$	none	$D_{555}H_{556}$
Ex15a-$W_{513}K/R_{546}K$	none[b]	$Q_{541}G_{542}$	none	$D_{555}H_{556}$

[a] Proteins modeled using the HMMSTR/ROSETTA Monte Carlo fragment insertion−folding program predict a β-sheet secondary structure for FMRP's RG-rich region with three to four turns (turns 1−4, N-terminal to C-terminal). Residue numbering is based on the full-length exon 15, Ex15a. [b] In this case there is no transition between α-helix and β-sheet.

Table 3: Effect of Mutations on the Helix Leading to the RG-Rich Region[a]

mutant protein	E_{523}	S_{524}	F_{525}	L_{526}	R_{527}	R_{528}
Ex15a	h[b]	h	h	h	h	h
Ex15b	h	h	h	h	h	h
Ex15c	h	−	−	−	h	−
Ex15a-$R_{507}K$	h	h	h	h	h	h
Ex15a-$R_{507}K/R_{546}K$	h	h	h	h	h	h
Ex15a-$W_{513}K$	h	h	h	h	h	−
Ex15a-$W_{513}K/R_{546}K$	h	h	h	h	h	h

[a] Proteins modeled using the HMMSTR/ROSETTA Monte Carlo fragment insertion−folding program predict an α-helix secondary structure leading up to FMRP's RG-rich region, except for Ex15c. Residue numbering is based on the exon 15a encoded protein. [b] h is helix; − is non-α-helix and non-β-sheet.

Ex15a-$W_{513}K$-$R_{546}K$ were prepared and analyzed. Modeling studies of the $W_{513}K$ mutant on an Ex15a background revealed that like the $R_{507}K$ mutant its β-sheet structure resembled the Ex15c protein, more than the Ex15a protein from which it was derived (Table 2). Posttranslational methylation kinetic studies of this mutant, akin to those shown in Figure 5A, showed that the methylation of the $W_{513}K$ mutant was reduced compared to Ex15a (Figure 8A). Similarly, the $W_{513}K/R_{546}K$ double mutant was very weakly methylated.

The substitution of an aromatic amino acid with a basic amino acid might be expected to alter the local protein structure. To assess the effect of a milder change of this residue on arginine methylation, we used a chemical modification approach. *N*-Bromosuccinimide (NBS) is a known modifier of tryptophan (*44*). Specifically, oxidation of tryptophan by NBS results in the formation of *N*-formylkynurenine (*53*). As this modification is more modest than lysine substitution and W_{513} is the only tryptophan in Ex15a, we determined whether its oxidation affected protein arginine methylation of the RG region. The results, in Figure 8B, show that arginine methylation was unaffected by prior treatment with NBS; nevertheless, under the same conditions, the oxidation of tryptophan in $FMRP_{498-513}$ (W_{513}) was readily measured as a loss of A_{280} absorbance. In contrast, a control peptide that lacked tryptophan was stable in the presence of NBS (Figure 8C).

Taken together, these data suggest that the loss of amino acid residues, as occurs from the use of alternative splice sites b and c, and amino acid substitutions within the N-terminal region of exon 15-encoded residues produce local alterations of the downstream RG-rich region that in turn lead to changes in arginine methylation.

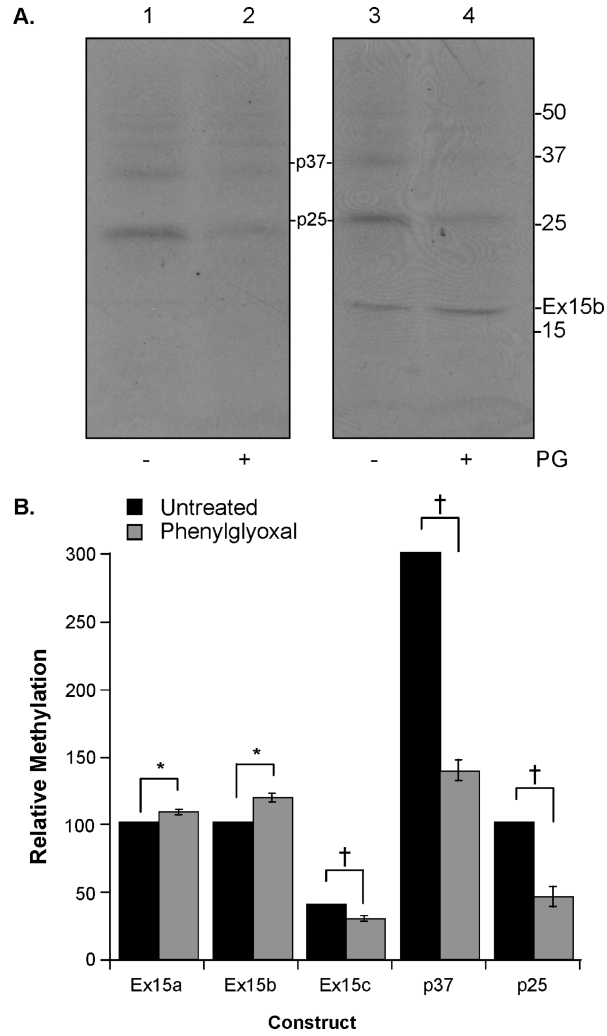

FIGURE 4: Phenylglyoxal treatment decreases methylation of Ex15c. (A) RRL (lanes 1 and 2) and RRL-produced Ex15b (lanes 3 and 4) were treated or not treated with 3% PG (as indicated) and were subsequently subjected to posttranslational *in vitro* methylation in the presence of ^{3}H-SAM. Endogenous RRL methylated proteins (p37 and p25) that are affected by PG treatment are indicated, as is Ex15b. (B) RRL-produced Ex15a, Ex15b, and Ex15c were treated or not treated with 3% PG as in (A). The intensity of untreated Ex15a methylation at 120 min was arbitrarily set to 100, and each of the treated and untreated proteins was normalized to it. Values for four to six reactions per protein are presented. Asterisks denote a significant increase in methylation $P < 0.0001$, one-way ANOVA, Scheffe's post hoc test; crosses denote a significant decrease in methylation $P < 0.0001$, one-way ANOVA, Scheffe's post hoc test. Note that at 120 min Ex15a methylation is saturated so the relative methylation of Ex15c appears greater; however, to detect the decrease due to PG, it was necessary to run the experiment in this way.

DISCUSSION

In this study we used a combination of molecular modeling, chemical modification, site-directed mutagenesis, and enzyme assays to investigate the effect exon 15-encoded residues had on the methylation of arginine residues in FMRP's RG-rich region. The study was prompted by prior work, which revealed that the three exon 15 alternatively spliced variants are differentially methylated *in vitro* (*31*). Modeling was performed on the C-terminal domain of FMRP

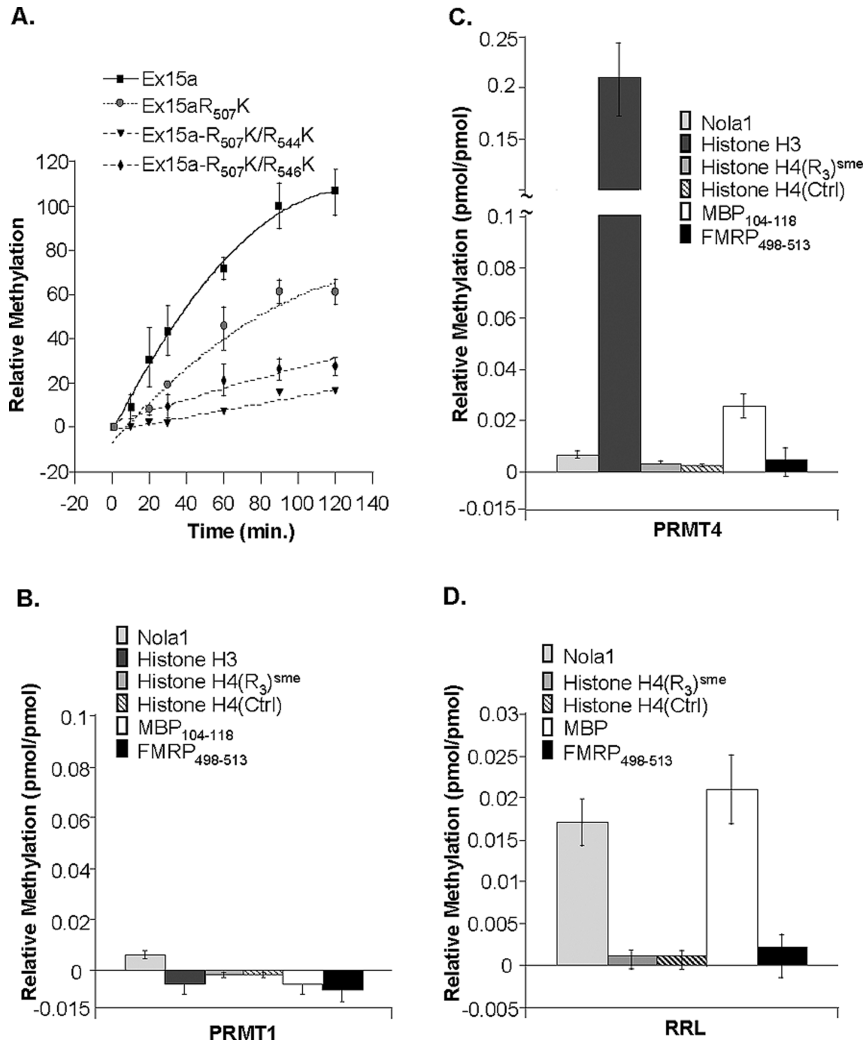

FIGURE 5: Posttranslational methylation of Ex15a-$R_{507}K$ truncation mutants is reduced *via* structural alteration of arginine residues in FMRP's RG-rich region. (A) Kinetics of posttranslational *in vitro* methylation of Ex15a, Ex15a-$R_{507}K$, Ex15a-$R_{507}K/R_{546}K$, and Ex15a-$R_{507}K/R_{544}K$ proteins. Values for three reactions per protein were normalized to the intensity of Ex15a methylation at 90 min (set to 100%). (B) Recombinant PRMT1 was incubated with proteins (Nola1, histone H3) and peptides (histone $H4(R_3)^{sme}$, H4(Ctrl), $MBP_{104-118}$, $FMRP_{498-513}$) in the presence of limiting ^{3}H-SAM, as described in Experimental Procedures. Filter counts minus background counts in the absence of the PRMT are plotted as $pmol_{incorporated}$/pmol ^{3}H-SAM. The results for four independent experiments for each substrate are plotted. (C) As in (B) except recombinant CARM1/PRMT4 was used. The results for four independent experiments for each protein/peptide at each amount of RRL are plotted. (D) RRL-dependent methylation of proteins (Nola1, MBP) and peptides (histone $H4(R_3)^{sme}$, H4(Ctrl), $FMRP_{498-513}$) was performed as in (B). The results for four independent experiments for each protein/peptide at each amount of RRL are plotted.

following a long-standing tradition of modeling various portions of this protein (*54–58*). Here, we used the HMMSTR/ROSETTA Monte Carlo fragment insertion−folding program to examine the effect deletions or amino acid substitutions had on the structure of the protein and especially the RG-rich domain. A variation of this program has been used to investigate the conformational changes that occur in the open and closed states of various K^+ ion channels (*59*). In the case of the open state of the Kv1.2 channel, whose crystal structure was previously determined, ROSETTA predicted a protein conformation with a root-mean-square deviation of <4 Å from the native protein. Moreover, in a test data set of 39 proteins ROSETTA models more accurately predicted the native backbone than a more widely used program, MODELER (*60*). Additionally, ROSETTA models had reasonably accurate side-chain conformations.

ROSETTA models of the exon 15 alternatively spliced FMRP variants and the assorted point mutants that were made predicted a common structural motif for the RG-rich region and its immediate C-terminal residues, i.e., a three to four strand antiparallel β-sheet. This feature is also present in several other RNA binding motifs including the cold shock domain (*61*), the RNP domain (*62*), and the double-stranded RNA-binding domain (*63*) where they create a surface rich in basic residues that are used to bind nucleic acids. Interestingly, the RG-rich region of nucleolin, another RNA binding protein, has been modeled as an extended β-spiral, or poly(L-proline) II helix on the basis of circular dichroism (CD) data (*64, 65*). However, although it harbors three RGG motifs, the RG-rich region of FMRP does not align well with the multiple RGGF repeats found in the consensus RGG-box sequence, of which nucleolin is a founding member (*66*). Thus, it is not surprising that the folds adopted by these two proteins differ.

Despite the structural similarities of the RG-rich regions of the Ex15 variant proteins, the other universal characteristic of the ROSETTA models was their plasticity. This was evidenced by the fact that the global conformation (Supporting Information Figure 2) and the local conformation of the RG-rich region antiparallel β-sheet of each of these

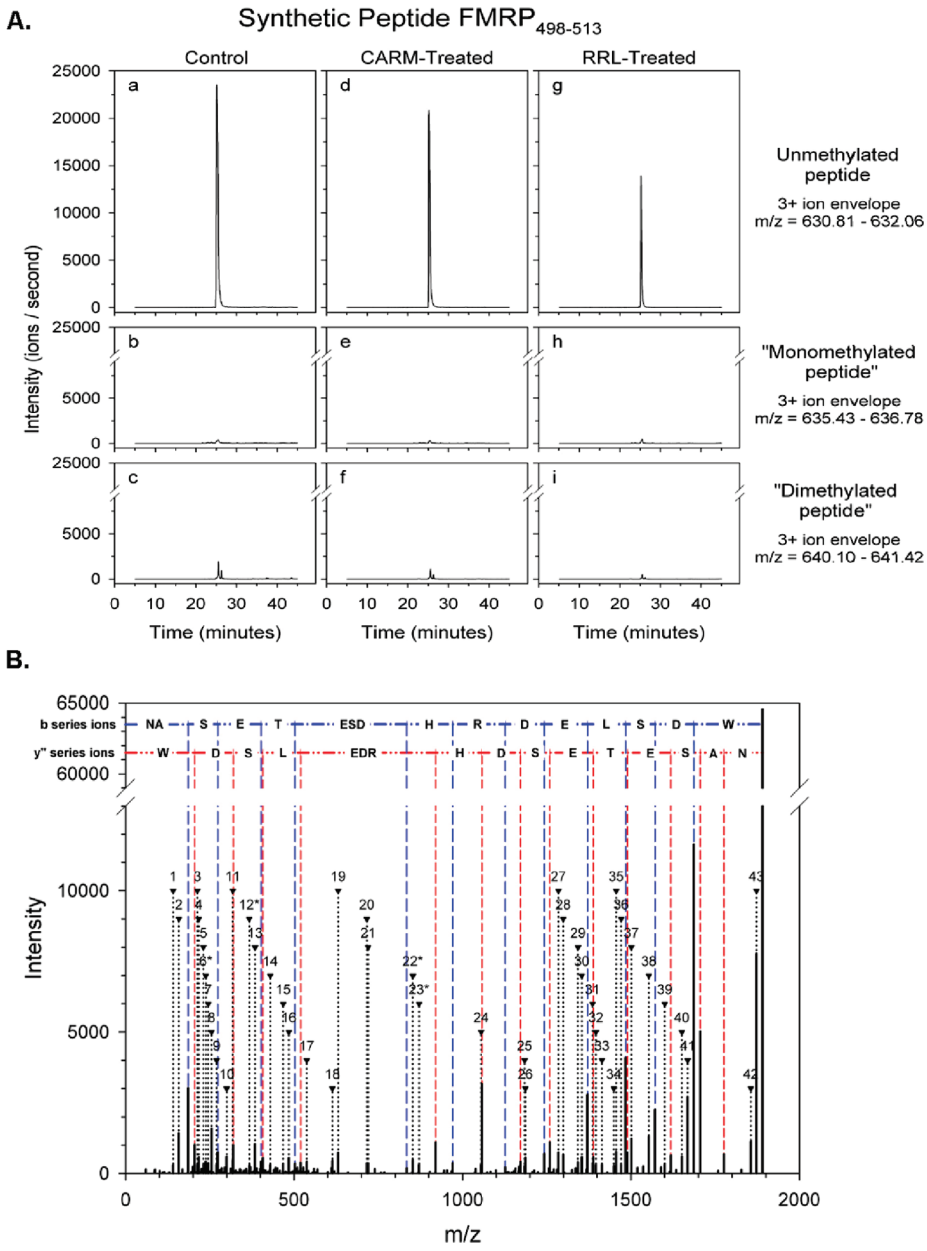

FIGURE 6: FMRP residue R_{507} is not methylated *in vitro*. (A) Methylation of $FMRP_{498-513}$ was performed in the presence of excess SAM (1250-fold molar excess over peptide) in the absence of any PRMT (a−c) or using recombinant PRMT4 (d−f) or RRL (g−i) as in Figure 5C,D. The peptides were recovered on C18 tips and subjected to mass spectrometry. The 3+ ion envelope for the unmethylated peptide (a, d, g), the monomethylated peptide (b, e, h), and the dimethylated peptide (c, f, i) are shown. (B) MS/MS spectrum of untreated $FMRP_{498-513}$ showing b and y″ series ions (blue dashed lines and red dashed lines, respectively). Approximately 2.5 pmol of the peptide was separated by LC, and MS/MS spectra were taken as described. While a substantial amount of the peptide remained intact (*m*/*z* 945.89 2+ ion corresponding to the 1890.77 1+ ion after transformation), the ion fragments produced in the MS/MS spectrum included 13 of 15 possible y″ ions and 12 of 14 possible b ions. Forty-three other ions with intensities greater than 250 ions total are shown in black and numbered 1 through 43. The identities of the marked ions are shown in Supporting Information Table 1.

proteins were highly disparate. Indeed, this feature was experimentally reflected in differences in the ability of each of the variants and mutants to be methylated *in vitro* (Figures 5A and 8A).

The premise behind the modeling studies was to use the data to obtain a clearer understanding of the mechanism by which alternative splicing influences arginine methylation. Thus, we tried to correlate data on the methylation of specific mutants with certain structural features of the models. One of these measures was solvent accessibility. Remarkably, the ROSETTA models showed the arginine residues in the RG-rich region of Ex15a and Ex15b to be relatively inaccessible to solvent. Consistent with this, we found that pretreating the proteins with the arginine-modifying reagent, phenylglyoxal, did not inhibit their downstream methylation (Figure 4). In contrast, the ROSETTA model of Ex15c predicted that R_{539}, R_{544}, and R_{546} would be slightly more solvent accessible than the corresponding residues in Ex15a or Ex15b. Indeed, we observed a decrease in Ex15c methylation following PG treatment. This effect has added significance given the fact that phenylglyoxal modification occurs on the neutral guanidine form of the arginyl side chain (*67*), and the p*I* of Ex15c is greater than that of Ex15a or Ex15b (11.0 vs 9.8 and 10.3, respectively). However, differential effects of PG on the PRMTs that modify Ex15a/b versus Ex15c cannot be discounted. Unfortunately, however, there was no obvious

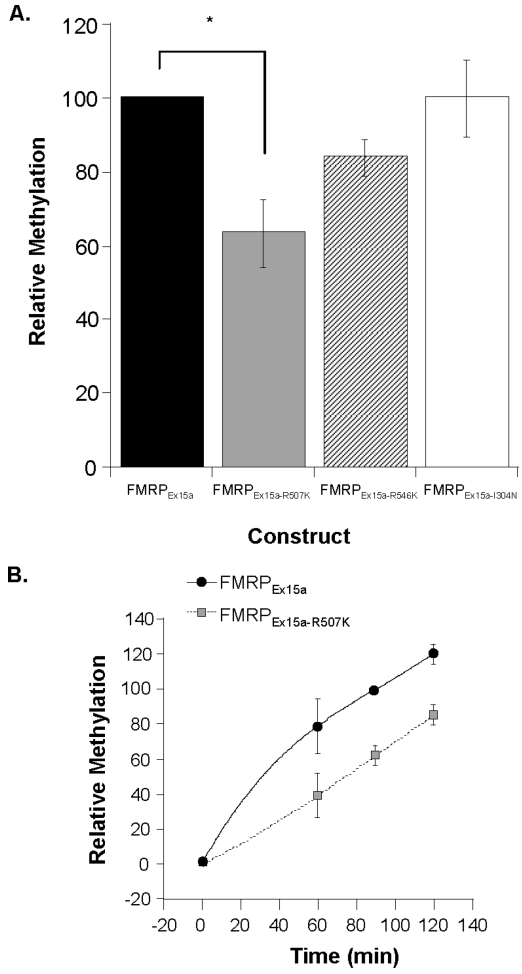

FIGURE 7: Reduced methylation of the FMRP$_{Ex15a-R507K}$ correlates with decreases observed in Ex15a-R_{507}K. Posttranslational *in vitro* methylation of FMRP$_{Ex15a-R507K}$, FMRP$_{Ex15a-R546K}$, and FMRP$_{Ex15a-I304N}$ normalized to FMRP$_{Ex15a}$ methylation at 90 min. The values represent the mean of three independent experiments of duplicate assays. Asterisk denotes $P < 0.0001$, one-way ANOVA, Scheffe's post hoc test. (B) Kinetics of posttranslational *in vitro* methylation of FMRP$_{Ex15a}$ and FMRP$_{Ex15a-R507K}$ proteins. Values for three reactions per protein were normalized to the intensity of FMRP$_{Ex15a}$ at 90 min (set to 100%).

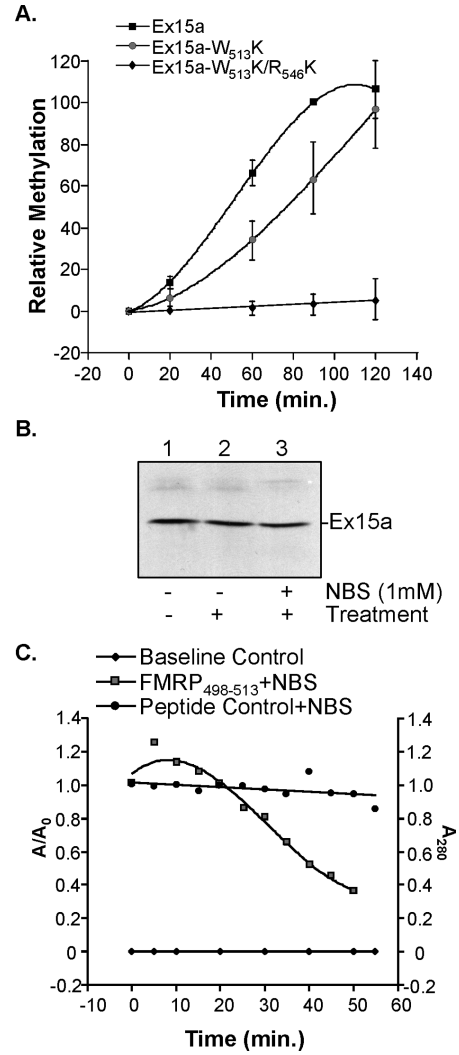

FIGURE 8: Mutating W_{513} also decreases FMRP arginine methylation. (A) Kinetics of posttranslational *in vitro* methylation of Ex15a, Ex15a-W_{513}K, and Ex15a-W_{513}K/R_{546}K proteins. Values for three reactions per protein were normalized to the intensity of Ex15a methylation at 90 min (set to 100%). (B) Ex15a treated (lane 3) or mock-treated (lane 2) with 1 mM NBS for 1 h was subjected to posttranslational *in vitro* methylation for 90 min. An untreated sample was used as a positive control (lane 1). The reactions were resolved by SDS−PAGE and subjected to fluorography. (C) FMRP$_{498-513}$ (squares) or a control peptide lacking W residues (circles) was added to a solution of 0.1 mM NBS. At the indicated times A_{280} values for each peptide were determined. The results were indexed to the A_{280} value immediately after the addition of the peptide (A/A_0). The diamonds show the A_{280} values of the NBS solution in the absence of peptide over the same period of time, demonstrating the stability of the spectrophotometer.

correlation between solvent accessibility and the individual R residues of the point and double point mutants that were made (Supporting Information Figure 3). We also noted that residues in the helix leading to the RG-rich region of the molecule were altered in the poorly methylated Ex15c splice variant. However, this feature was not recapitulated in any of the other mutant proteins that were examined, and thus it is unlikely to be the defining cause of the decreased methylation seen in Ex15c. On the other hand, ROSETTA models of Ex15c, Ex15a-R_{507}K, and Ex15a-W_{513}K predicted a smaller first strand of the antiparallel β-sheet than the wild-type Ex15a variant. While the significance of this is not known, it does result in residues $R_{532-534}$ being in an unstructured turn, which may preclude their methylation.

Sites of arginine methylation in proteins are sometimes identified through the use of point mutations, which are not modified by PRMTs. For example, systematic R-K mutations in p53 binding protein 1 (53BP1) led to the conclusion that R_{1398}, R_{1400}, and R_{1401} are important methyltransferase targets in this protein (*68*). Likewise, it was inferred from R-K mutations in the yeast hnRNP, Hrp1p, that R_{516} and R_{519} were methylated, while R_{343} was not modified (*69*). With regard to FMRP, Stetler et al. concluded from methylation studies of a series of single and multiple FMRP arginine mutants that several residues within the RG-rich region were methylated (*33*). These data agreed qualitatively with *in vitro* methylation studies comparing Ex15a-R_{544}K and Ex15a-R_{546}K mutant proteins to Ex15a (*31*) and with a peptide methylation study using partially purified rat brain PRMT (*48*). Based on the structural data presented here, however, it is not clear whether the decreased methylation of the RG-rich region mutants is due to loss of methylation at the mutation site or due to a decreased ability to methylate other arginine residues in the region, or both. Future mass

spectrometry studies should address this point. Nevertheless, it is clear that the diminished methylation accompanying the $R_{507}K$ mutation is solely due to structural perturbations in the arginine residues in the RG-rich region that are methylated, rather than the loss of methylation at position 507 (Figures 5 and 6). Furthermore, it is also apparent that this perturbation, which partially mimics the loss of the first 25 amino acids encoded by FMR1 exon 15, is recapitulated in full-length FMRP. These results, coupled with previous data showing similar methylation decreases in the full-length and truncated forms of exon 15c, indicate that FMRP's C-terminal domain acts as an independent unit. These data are further strengthened by comparable results for full-length and truncated $FMRP_{Ex15a\text{-}R546K}$ and by the lack of change the $I_{304}N$ mutation had on methylation *in vitro* (Figure 7).

The expression of the three FMR1 exon 15 isoforms (*47*) implies that they all have a physiological relevance. To date, all of the published functional studies have focused on the effect phosphorylation of the exon 15a variant has on translation and synapse dynamics (*35, 70*). However, the disparity between the methylation of $FMRP_{Ex15a}$ and $FMRP_{Ex15c}$ suggests that interactions between exon 15-encoded N-terminal residues with one or more proteins may provide a means of differentially controlling the methylation state of the RG-rich region. In turn, this may influence the interaction of G-quartet-containing mRNAs (*71–73*) with the RG-rich region. One candidate interacting protein that may be relevant in this regard is microspherule protein 58 (MSP58), which binds to residues 490−526 of $FMRP_{Ex15a}$ (*74*) (Figure 1B). Such control may be absent or impaired in $FMRP_{Ex15c}$ as the region overlapping the MSP58 binding site is much smaller than in $FMRP_{Ex15a}$. Studies are currently underway to determine this. Nevertheless, it is clear from the present work that the conformation of exon 15-encoded residues plays an important role in the methylation of FMRP's RG-rich region.

ACKNOWLEDGMENT

We thank Drs. W. T. Brown and David L. Miller for helpful discussions concerning the manuscript.

SUPPORTING INFORMATION AVAILABLE

Figures 1−5 and Tables 1 and 2 showing the expression of the FMRP exon 15 alternatively spliced variants and mutants used in this study, HMMSTR/ROSETTA models of these proteins, the predicted solvent accessibility of their RG-rich region arginine residues, and the identification of dimethylarginine by mass spectroscopy. This material is available free of charge via the Internet at http://pubs.acs.org.

REFERENCES

1. Scebba, F., De Bastiani, M., Bernacchia, G., Andreucci, A., Galli, A., and Pitto, L. (2007) PRMT11: a new Arabidopsis MBD7 protein partner with arginine methyltransferase activity. *Plant J. 52*, 213–222.
2. Sharmistha Pal, S. S. (2007) Interplay between chromatin remodelers and protein arginine methyltransferases. *J. Cell. Physiol. 213*, 306–315.
3. Zhang, X., Zhou, L., and Cheng, X. (2000) Crystal structure of the conserved core of protein arginine methyltransferase PRMT3. *EMBO J. 19*, 3509–3519.
4. Lee, D. Y., Ianculescu, I., Purcell, D., Zhang, X., Cheng, X., and Stallcup, M. R. (2007) Surface-scanning mutational analysis of protein arginine methyltransferase 1: roles of specific amino acids in methyltransferase substrate specificity, oligomerization, and coactivator function. *Mol. Endocrinol. 21*, 1381–1393.
5. Jin, P., Zarnescu, D. C., Zhang, F., Pearson, C. E., Lucchesi, J. C., Moses, K., and Warren, S. T. (2003) RNA-mediated neurodegeneration caused by the fragile X premutation rCGG repeats in Drosophila. *Neuron 39*, 739–747.
6. Lim, Y., Kwon, Y.-H., Won, N. H., Min, B.-H., Park, I.-S., Paik, W. K., and Kim, S. (2005) Multimerization of expressed protein-arginine methyltransferases during the growth and differentiation of rat liver. *Biochim. Biophys. Acta 1723*, 240–247.
7. Pal, S., Viswanath, S. N., Erdjument-Bromage, H., Tempst, P., and Sif, S. (2004) Human SWI/SNF-associated PRMT5 methylated histone H3 arginine 8 and negatively regulates expression of ST7 and NM23 tumor suppressor genes. *Mol. Cell. Biol. 24*, 9630–9645.
8. Passeri, D., Marcucci, A., Rizzo, G., Billi, M., Panigada, M., Leonardi, L., Tirone, F., and Grignani, F. (2006) Btg2 enhances retinoic acid-induced differentiation by modulating histone H4 methylation and acetylation. *Mol. Cell. Biol. 26*, 5023–5032.
9. Yoshimoto, T., Boehm, M., Olive, M., Crook, M. F., San, H., Langenickel, T., and Nabel, E. G. (2006) The arginine methyltransferase PRMT2 binds RB and regulates E2F function. *Exp. Cell Res. 312*, 2040–2053.
10. Strahl, B. D., Briggs, S., Brame, C. J., Caldwell, J. A., Koh, S. S., Ma, T., Cook, J. R., Shabanowitz, J., Hunt, D., Stallcup, M. R., and Allis, C. D. (2001) Methylation of histone H4 at arginine 3 occurs in vivo and is mediated by the nuclear receptor coactivator PRMT1. *Curr. Biol. 11*, 996–1000.
11. Sarmento, O. F., Digilio, L. C., Wang, Y., Perlin, J., Herr, J. C., Allis, C. D., and Coonrod, S. A. (2004) Dynamic alterations of specific histone modifications during early murine development. *J. Cell Sci. 117*, 4449–4459.
12. Ancelin, K., Lange, U. C., Hajkova, P., Schneider, R., Bannister, A. J., Kouzarides, T., and Surani, M. A. (2006) Blimp1 associates with Prmt5 and directs histone arginine methylation in mouse germ cells. *Nat. Cell Biol. 8*, 623–630.
13. Wang, X., Zhang, Y., Ma, Q., Zhang, Z., Xue, Y., Bao, S., and Chong, K. (2007) SKB1-mediated symmetric dimethylation of histone H4R3 controls flowering time in Arabidopsis. *EMBO J. 26*, 1934–1941.
14. Le Guezennec, X., Vermeulen, M., Brinkman, A. B., Hoeijmakers, W. A. M., Cohen, A., Lasonder, E., and Stunnenberg, H. G. (2006) MBD2/NuRD and MBD3/NuRD, two distinct complexes with different biochemical and functional properties. *Mol. Cell. Biol. 26*, 843–851.
15. Aoki, K., Ishii, Y., Matsumoto, K., and Tsujimoto, M. (2002) Methylation of Xenopus CIRP2 regulates its arginine- and glycine-rich region-mediated nucleocytoplasmic distribution. *Nucleic Acids Res. 30*, 5182–5192.
16. Bedford, M. T., Frankel, A., Yaffe, M. B., Clarke, S., Leder, P., and Richard, S. (2000) Arginine methylation inhibits the binding of proline-rich ligands to Src homology 3, but not WW, domains. *J. Biol. Chem. 275*, 16030–16036.
17. Belyanskaya, L. L., Gehrig, P. M., and Gehring, H. (2001) Exposure on cell surface and extensive arginine methylation of Ewing Sarcoma (EWS) protein. *J. Biol. Chem. 276*, 18681–18687.
18. Cote, J., Boisvert, F.-M., Boulanger, M.-C., Bedford, M. T., and Richard, S. (2003) Sam68 RNA binding protein is an in vivo substrate for protein arginine N-methyltransferase 1. *Mol. Biol. Cell 14*, 274–287.
19. Green, D. M., Marfatia, K. A., Crafton, E. B., Zhang, X., Cheng, X., and Corbett, A. H. (2002) Nab2p is required for poly(A) RNA export in *Saccharomyces cerevisiae* and is regulated by arginine methylation *via* Hmt1p. *J. Biol. Chem. 277*, 7752–7760.
20. Lee, J., and Bedford, M. T. (2002) PABP1 identified as an arginine methyltransferase substrate using high-density protein arrays. *EMBO Rep. 3*, 268–273.
21. Liu, Q., and Dreyfuss, G. (1995) In vivo and in vitro arginine methylation of RNA binding proteins. *Mol. Cell. Biol. 15*, 2800–2808.
22. McBride, A. E., Cook, J. T., Stemmler, E. A., Rutledge, K. L., McGrath, K. A., and Rubens, J. A. (2005) Arginine methylation of yeast mRNA-binding protein Npl3 directly affects its function, nuclear export, and intranuclear protein interactions. *J. Biol. Chem. 280*, 30888–30898.
23. Herrmann, F., Bossert, M., Schwander, A., Akgun, E., and Fackelmayer, F. O. (2004) Arginine methylation of scaffold

attachment factor A (SAF-A) by hnRNP-particle associated PRMT1. *J. Biol. Chem. 279*, 48774–46779.
24. Rho, J., Choi, S., Seong, Y. R., Choi, J., and Im, D.-S. (2001) The arginine-1493 residue in QRRGRTGR1493G motif IV of the hepatitis C virus NS3 helicase domain is essential for NS3 protein methylation by the protein arginine methyltransferase 1. *J. Virol. 75*, 8031–8044.
25. Siomi, H., Choi, M., Siomi, M. C., Nussbaum, R. L., and Dreyfuss, G. (1994) Essential role for KH domains in RNA binding: impaired RNA binding by a mutation in the KH domain of FMR1 that causes fragile X syndrome. *Cell 77*, 33–39.
26. Siomi, H., Siomi, M. C., Nussbaum, R. L., and Dreyfuss, G. (1993) The protein product of the fragile X gene, FMR1, has characteristics of an RNA-binding protein. *Cell 74*, 291–298.
27. Bedford, M. T., and Richard, S. (2005) Arginine methylation: an emerging regulatorof protein function. *Mol. Cell 18*, 263–272.
28. Boisvert, F.-M., Chenard, C. A., and Richard, S. (2005) Protein interfaces in signaling regulated by arginine methylation, Sci. STKE. (www.stke.org/cgi/content/full/sigtrans;2005/271/re2, 1−10).
29. Denman, R. B. (2002) Methylation of the arginine-glycine-rich region in the fragile X mental retardation protein FMRP differentially affects RNA binding. *Cell. Mol. Biol. Lett. 7*, 877–883.
30. Dolzhanskaya, N., Merz, G., Aletta, J. M., and Denman, R. B. (2006) Methylation regulates FMRP's intracellular protein-protein and protein-RNA interactions. *J. Cell. Sci. 119*, 1933–1946.
31. Dolzhanskaya, N., Merz, G., and Denman, R. B. (2006) Alternative splicing modulates PRMT-dependent methylation of FMRP. *Biochemistry 45*, 10385–10393.
32. Duan, P., Xu, Y., Birkaya, B., Myers, J., Pelletier, M., Read, L. K., Guarnaccia, C., Pongor, S., Denman, R. B., and Aletta, J. M. (2007) Generation of polyclonal antiserum for the detection of methylarginine proteins. *J. Immunol. Methods 320*, 132–142.
33. Stetler, A., Winograd, C., Sayegh, J., Cheever, A., Patton, E., Zhang, Z., Clarke, S., and Ceman, S. (2006) Identification and characterization of the methyl arginines in the fragile X mental retardation protein Fmrp. *Hum. Mol. Genet. 15*, 87–96.
34. Siomi, M. C., Higashijima, K., Ishizuka, A., and Siomi, H. (2002) Casein kinase II phosphorylates the fragile X mental retardation protein and modulates its biological properties. *Mol. Cell. Biol. 22*, 8438–8447.
35. Ceman, S., O'Donnell, W. T., Reed, M., Patton, S., Pohl, J., and Warren, S. T. (2003) Phosphorylation influences the translation state of FMRP-associated polyribosomes. *Hum. Mol. Genet. 12*, 3295–3305.
36. Hsu, I.-W., Hsu, M., Li, C., Chuang, T.-W., Lin, R.-I., and Tarn, W.-Y. (2005) Phosphorylation of Y14 modulates its interaction with proteins involved in mRNA metabolism and influences its methylation. *J. Biol. Chem. 280*, 34507–34512.
37. Yun, C. Y., and Fu, X.-D. (2000) Conserved SR protein kinase functions in nuclear import and its action is counteracted by arginine methylation in Saccharomyces cerevisiae. *J. Cell Biol. 150*, 707–718.
38. Denman, R. B., Dolzhanskaya, N., and Sung, Y.-J. (2004) Regulating a translational regulator: mechanisms cells use to control the activity of the fragile X mental retardation protein. *Cell. Mol. Life Sci. 61*, 1714–1728.
39. Denman, R. B. (2006) in Sci. STKE (e-letter pp http://stke.sciencemag.org/cgi/eletters/sigtrans;2001/93/pl1).
40. Sung, Y.-J., Dolzhanskaya, N., Nolin, S. L., Brown, W. T., Currie, J. R., and Denman, R. B. (2003) The fragile X mental retardation protein FMRP binds elongation factor 1A mRNA and negatively regulates its translation in vivo. *J. Biol. Chem. 278*, 15669–15678.
41. Denman, R. B., and Sung, Y.-J. (2002) Species-specific and isoform-specific RNA binding of human and mouse fragile X mental retardation proteins. *Biochem. Biophys. Res. Commun. 292*, 1063–1069.
42. Cimato, T. R., Tang, J., Xu, Y., Guarnaccia, C., Herschman, H. R., Pongor, S., and Aletta, J. M. (2002) Nerve growth factor-mediated increases in protein methylation occur predominantly at type I arginine methylation sites and involve protein arginine methyltransferase 1. *J. Neurosci. Res. 67*, 435–442.
43. Savitzky, A., and Golay, M. J. E. (1964) Smoothing and differentiation of data by simplified least squares procedures. *Anal. Chem. 36*, 1627–1639.
44. Petrova, S. D., Bakalova, N. G., and Kolev, D. N. (2006) Catalytically important amino acid residues in endoglucanases from a mutant strain Trichoderma sp. M7. *Biochemistry (Moscow) 71*, S25–S30.
45. Takahashi, K. (1968) The reaction of phenylglyoxal with arginine residues in proteins. *J. Biol. Chem. 243*, 6171–6179.
46. Verkerk, A. J., de Graaff, E., De Boulle, K., Eichler, E. E., Konecki, D. S., Reyniers, E., Manca, A., Poustka, A., Willems, P. J., Nelson, D. L., and Oostra, B. (1993) Alternative splicing in the fragile X gene FMR1. *Hum. Mol. Genet. 2*, 399–404.
47. Ashley, C. T., Sutcliffe, J. S., Kunst, C. B., Leiner, H. A., Eichler, E. E., Nelson, D. L., and Warren, S. T. (1993) Human and murine FMR-1: alternative splicing and translational initiation downstream of the CGG-repeat. *Nat. Genet. 4*, 244–251.
48. Ai, L. S., Lin, C. H., Hsieh, M., and Li, C. (1999) Arginine methylation of a glycine and arginine rich peptide derived from sequences of human FMRP and fibrillarin. *Proc. Natl. Sci. Counc. Repub. China B 23*, 175–180.
49. Najbauer, J., Johnson, B. A., Young, A. L., and Aswad, D. W. (1993) Peptides with sequences similar to glycine, arginine-rich motifs in proteins interacting with RNA are efficiently recognized by methyltransferase(s) modifying arginine in numerous proteins. *J. Biol. Chem. 268*, 10501–10509.
50. Whitehead, S. E., Jones, K. W., Zhang, X., Cheng, X., Terns, R. M., and Terns, M. P. (2002) Determinants of the interaction of the spinal muscular atrophy disease protein SMN with the dimethylarginine-modified box H/ACA small nucleolar ribonucleoprotein GAR1. *J. Biol. Chem. 277*, 48087–48093.
51. McBride, A. E. (2006) Diverse roles of protein arginine methyltransferases, in *The Enzymes*, pp 51−103, Elsevier, San Diego.
52. De Boulle, K., Verkerk, A. J., Reyniers, E., Vits, L., Hendrickx, J., Van Roy, B., Van den Bos, F., de Graaff, E., Oostra, B. A., and Willems, P. J. (1993) A point mutation in the FMR-1 gene associated with fragile X mental retardation. *Nat. Genet. 3*, 31–35.
53. Taylor, S. W., Fahy, E., Murray, J., Capaldi, R. A., and Ghosh, S. S. (2003) Oxidative post-translational modification of tryptophan residues in cardiac mitochondrial proteins. *J. Biol. Chem. 278*, 19587–19590.
54. Musco, G., Kharrat, A., Stier, G., Faternali, F., Gibson, T. J., Nilges, M., and Pastore, A. (1997) The solution structure of the first KH domain of FMR1, the protein responsible for the fragile X syndrome. *Nat. Struct. Biol. 4*, 712–716. [erratum (1997) *Nat. Struct. Biol.* Oct 4(10), 840].
55. Adinolfi, S., Bagni, C., Musco, G., Gibson, T., Mazzarella, L., and Pastore, A. (1999) Dissecting FMR1, the protein responsible for fragile X syndrome, in its structural and functional domains. *RNA 5*, 1248–1258.
56. Ramos, A., Hollingsworth, D., Adinolfi, S., Castets, M., Kelly, G., Frenkiel, T. A., Bardoni, B., and Pastore, A. (2006) The structure of the N-terminal domain of the fragile X mental retardation protein: a platform for protein-protein interaction. *Structure 14*, 21–31.
57. Valverde, R., Pozdnyakova, I., Kajander, T., Venkatraman, J., and Regan, L. (2007) Fragile X mental retardation syndrome: structure of the KH1-KH2 domains of fragile X mental retardation protein. *Structure 15*, 1090–1098.
58. Pozdnyakova, I., and Regan, L. (2005) New insights into Fragile X syndrome. Relating genotype to phenotype at the molecular level. *FEBS J. 272*, 872–878.
59. Yarov-Yarovoy, V., Baker, D., and Catterall, W. A. (2006) Voltage sensor conformations in the open and closed states in ROSETTA structural models of K^+ channels. *Proc. Natl. Acad. Sci. U.S.A. 103*, 7292–7297.
60. Misura, K. M. S., Chivian, D., Rohl, C. A., Kim, D. E., and Baker, D. (2006) Physically realistic homology models built with ROSETTA can be more accurate than their templates. *Proc. Natl. Acad. Sci. U.S.A. 103*, 5361–5366.
61. Schindelin, H. M. M., and Heinemann, U. (1993) Universal nucleic acid-binding domain revealed by crystal structure of the B. subtilis major cold-shock protein. *Nature 364*, 164–168.
62. Katahira, M., Miyanoiri, Y., Enokizono, Y., Matsuda, G., Nagata, T., Ishikawa, F., and Uesugi, S. (2001) Structure of the C-terminal RNA-binding domain of hnRNP D0 (AUF1), its interactions with RNA and DNA, and change in backbone dynamics upon complex formation with DNA. *J. Mol. Biol. 311*, 973–988.
63. Nanduri, S., Carpick, B. W., Yang, Y., Williams, B. R. G., and Qin, J. (1998) Structure of the double-stranded RNA-binding domain of the protein kinase PKR reveals the molecular basis of its dsRNA-mediated activation. *EMBO J. 17*, 5458–5465.
64. Manival, X., Ghisolfi-Nieto, L., Joseph, G., Bouvet, P., and Erard, M. (2001) RNA-binding strategies common to cold-shock domain-

and RNA recognition motif-containing proteins. *Nucleic Acids Res. 29*, 2223–2233.

65. Ghisolfi, L., Joseph, G., Amalric, F., and Erard, M. (1992) The glycine-rich domain of nucleolin has an unusual supersecondary structure responsible for its RNA-helix-destabilizing properties. *J. Biol. Chem. 267*, 2955–2959.
66. Redish, L., Shen, J., Currie, J. R., and Denman, R. B. (2004) The RGG box: a domain in search of a consensus. *Curr. Top. Biochem. Res. 6*, 93–109.
67. Bjerrum, P. J., Wieth, J. O., and Borders, C. L. (1983) Selective phenylglyoxalation of functionally essential arginine residues in the erythrocyte anion transport protein. *J. Gen. Physiol. 81*, 453–484.
68. Adams, M. M., Wang, B., Xia, Z., Morales, J., Lu, X., Donehower, L. A., Bochar, D. A., Elledge, S. J., and Carpenter, P. B. (2005) 53BP1 oligomerization is independent of its methylation by PRMT1. *Cell Cycle 4*, 1854–1861.
69. Xu, C., and Henry, M. F. (2004) Nuclear export of hnRNP Hrp1p and nuclear export of hnRNP Npl3p are linked and influenced by the methylation state of Npl3p. *Mol. Cell. Biol. 24*, 10742–10756.
70. Pfeiffer, B. E., and Huber, K. M. (2007) Fragile X mental retardation protein induces synapse loss through acute postsynaptic translational regulation. *J. Neurosci. 27*, 3120–3130.
71. Darnell, J. C., Jensen, K. B., Jin, P., Brown, V., Warren, S. T., and Darnell, R. B. (2001) Fragile X mental retardation protein targets G quartet mRNAs important for neuronal function. *Cell 107*, 489–499.
72. Ramos, A., Hollingworth, D., and Pastore, A. (2003) G-quartet-dependent recognition between the FMRP RGG box and RNA. *RNA 9*, 1198–1207.
73. Menon, L., and Mihailescu, M.-R. (2007) Interactions of the G quartet forming semaphorin 3F RNA with the RGG box domain of the fragile X protein family. *Nucleic Acids Res. 35*, 5379–5382.
74. Davidovic, L., Bechara, E., Gravel, M., Jaglin, X. H., Tremblay, S., Sik, A., Bardoni, B., and Khandjian, E. W. (2006) The nuclear microSpherule protein 58 is a novel RNA-binding protein that interacts with fragile X mental retardation protein in polyribosomal mRNPs from neurons. *Hum. Mol. Genet. 15*, 1525–1538.
75. Eichler, E. E., Richards, S., Gibbs, R. A., and Nelson, D. L. (1994) Fine structure of the human FMR1 gene. *Hum. Mol. Genet. 3*, 684–685.

BI702298F